Geomechanics and Engineering, *Vol. 27, No. 4 (2021) 391-404*
https://doi.org/10.12989/gae.2021.27.4.391

Gob-side entry stability analysis by global-finite and local-discrete modeling approach

Pengfei Guo*[1,2], Yongxu Zhao[1], Yadi Yuan[1], Kengkeng Ye[1], Haijiang Zhang[1] and Qing Gao[1]

[1]*Key School of Civil Engineering, Shaoxing University, Shaoxing 312000, China*
[2]*State Key Laboratory for GeoMechanics and Deep Underground Engineering, China University of Mining & Technology, Beijing 100083, China*

(Received November 10, 2020, Revised October 9, 2021, Accepted October 13, 2021)

Abstract. In geotechnical engineering, the accurate evaluation of large-scale geotechnical engineering schemes before construction is very important. So the reliability of the surrounding rock support of the gob-side entry directly determines the success or failure of the gob-side entry remaining. To accurately evaluate designs of large scale engineering before the implementation, such as the gob-side entry retaining formed by roof cut and pressure releasing, this paper used the 3D finite element global model to obtain the local stress of the roadway surrounding rock. And then the local stress was applied as the boundary condition to the 3D discrete element roadway model to evaluate supporting effects of different support schemes during the gob-side entry retaining. Besides, based on numerical simulation, the coordinated support scheme of "constant resistance and large deformation cable + steel bolt + hydraulic prop + steel beam + U-shaped steel" was further proposed. The field test results shown that the support scheme can effectively control the deformation of the surrounding rock of the gob-side entry. The numerical simulation results were in good agreement with the field test results. So the feasibility and reliability of the numerical simulation evaluation method were verified by the field test results. Therefore, the global-finite and local-discrete modeling approach can be applied to mines that will implement the technology of the gob-side entry retaining formed by roof cut and pressure releasing, providing important references for the evaluation and optimization of its support design, and the determination of the dynamic pressure zone length.

Keywords: global-finite element; gob-side entry; local-discrete element; roof cut and pressure releasing; roadway surrounding rock deformation; stability analysis

1. Introduction

The non-chain-pillar longwall mining method has been widely studied and applied in recent years for its advantage of relaxing the imbalance of stripping and continuous mining, improving the economic benefit and recovery, etc (Bai *et al*. 2015). However, due to the different hydrogeological conditions, mining methods, support methods and construction techniques in different mining areas, it is difficult to analyze the gate stability before gob-side entry retaining. More importantly, in the whole life cycle of the gate, because the gob-side entry has to undergo severe disturbance of multiple mining stresses, so it is very necessary to analyze gate stability and optimize the original support design, the temporary support design before the gob-side entry retaining (Qin *et al.* 2020). It's worth noting that the structure and stress of the gate surrounding rock are instability before overlying strata stop moving for advancing mining. So large deformation or surrounding rock failure or collapse may occur at any time if error structural analysis of surrounding rock and unreasonable supporting design is used in gob-side entry retaining. Therefore, the research on stability analysis of surrounding rock in the gob-side entry is essential to ensure product safety and economic efficiency (Cheng *et al.* 2019, Valliappan *et al.* 2019, De Silva *et al.* 2019).

In recent years, many scholars have completed a lot of research on roadway support design, roadway deformation mechanism, roadway stability analysis and control, and anchor bolt and cable anchoring performance, and achieved a lot of valuable results (Huang *et al.* 2018, Bednarek and Majcherczyk. 2020). However, most of the existing researches focus on traditional coal mining methods such as room and pillar mining method, longwall mining method with coal pillars, and roadside packing without the coal pillar mining method. Moreover, due to the large range of stope simulation, discrete element software modeling and calculation takes a long time (Basarir *et al.* 2015, Valliappan *et al.* 2019). Therefore, finite element software is currently used to analyze the stability of roadways along goafs. But, due to a large number of joints and cracks in the surrounding rock of the goaf roadway under the influence of mining stress, it is difficult to solve the problem comprehensively and accurately by using finite element software (Zhang *et al.* 2018, Xie *et al.* 2020). So the accuracy of results of the numerical simulation using the finite element software is greatly compromised.

Because the surrounding rock of the roadway has to experience many times of severe mining stress during the gob-side entry retaining formed by roof cut and pressure

*Corresponding author, Ph.D.
E-mail: gpf20101989@163.com

ISSN: 2005-307X (Print), 2092-6219 (Online)

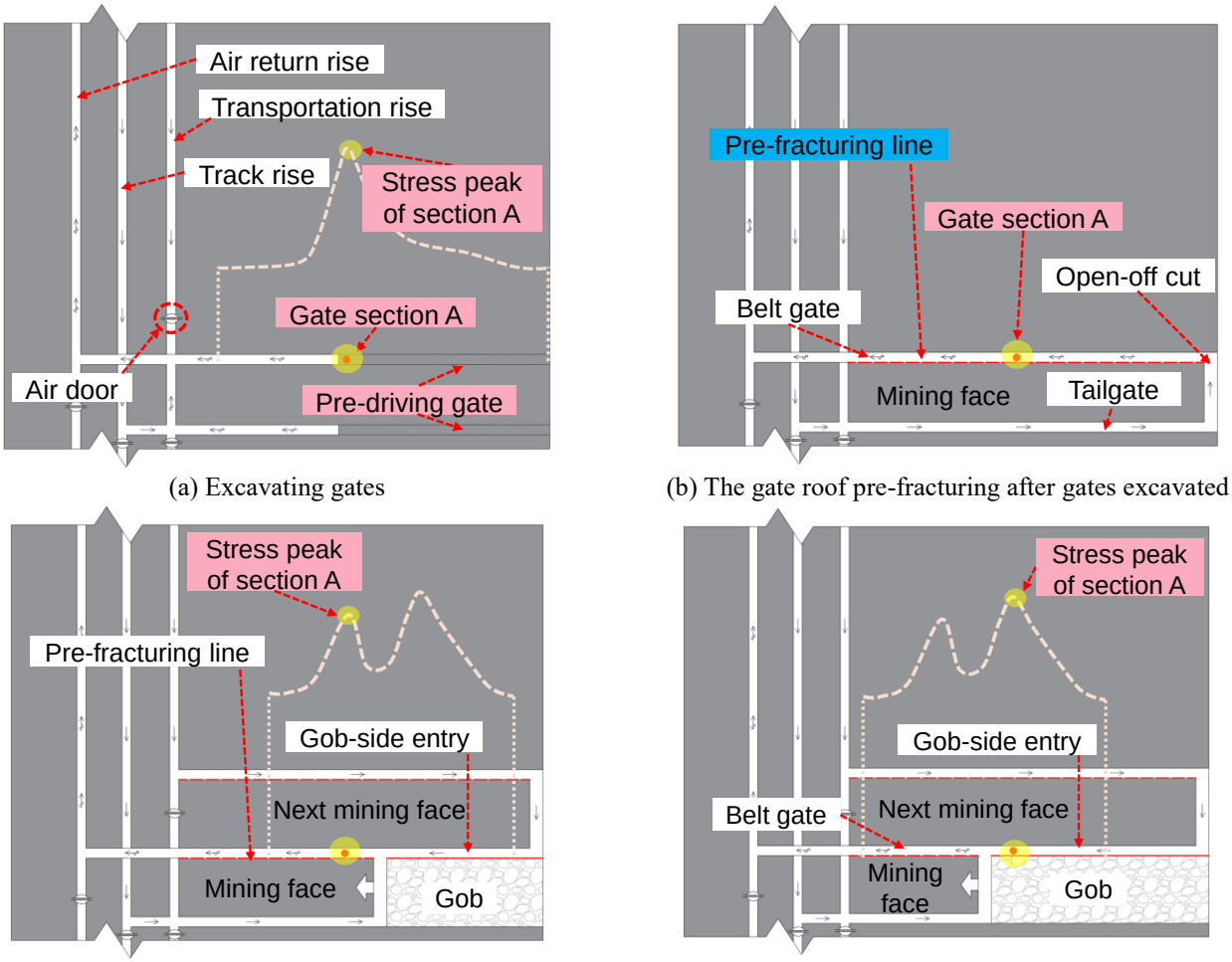

(a) Excavating gates

(b) The gate roof pre-fracturing after gates excavated

(c) The working face mining when the section A advanced working face

(d) The working face mining when the section A lagged the working face

Fig. 1 Process characteristics of the gob-side entry retaining formed by roof pre-fracturing

releasing (GEFRC), for example, stress disturbance for gate excavating, advancing disturbance for working face mining, and stress disturbance for advancing mining (see Fig. 1), the support design of the roadway should be considered from the perspective of the whole life cycle in the early stage of roadway excavation (Aksoy *et al.* 2013, Wang *et al.* 2017, Wu *et al.* 2019). With the rapid development of computer technology, numerical simulation technology has attracted more and more attention from engineering circles and researchers. Finite element software represented by ANSYS, ADINA, COMSOL Multiphysics, etc. has been widely used in engineering fields such as bridges, tunnels, buildings, and blasting (Zhu *et al*. 2019). FLAC3D based on the Finite Difference Method has a wide range of advantages such as display solution, fast calculation speed, accuracy and reasonableness. Therefore, it has been widely used in the stability analysis and optimization design of tunnels excavating and support design in the field of geotechnical engineering (Kim *et al.* 2018, Tan *et al.* 2019). However, in geotechnical engineering, most of the problems encountered are non-continuum. With the action of excavation, support and other engineering disturbances, the rock would fracture, rotate, sink and collapse, which will cause damage to the rock mass. And it is particularly important for rock stability analysis. For discrete element software such as UDEC, 3DEC, and PFC-3D, although they can perform numerical calculations on rock mass destruction, the calculation speed is often severely affected by the large range of rock mass and the huge number of units (Yin *et al.* 2020). For the technology of the GEFRC, not only the range of rock strata involved is very large, but also after the working face is mined, the overlying rock strata in the gob continuously undergoes rotational deformation, fracture, and collapse. So the finite element software or discrete element software cannot quickly and accurately complete the numerical calculation. Therefore, according to the technological characteristics of the GEFRC, the gob-side entry stability analysis by a global-finite and local-discrete modeling approach is proposed.

To study the deformation mechanism, the stress distribution law, and the rationality of roadway support design in the roadway life cycle before gob-side entry retaining, theoretical analysis and numerical simulation are comprehensively used in this paper. Because the surrounding rock structure and its stability of the roadway during the gob-side entry retaining is the key to the roadway

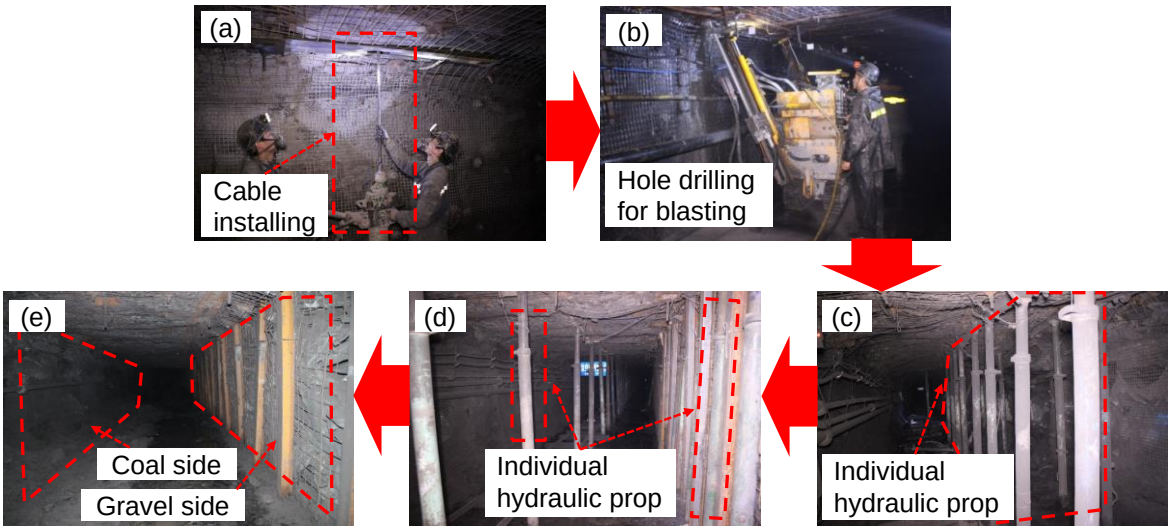

Fig. 2 Technological process of gob-side entry formed by roof cut: (a) Installing the constant resistance and large deformation cables before roof pre-fracturing; (b) The hole drilling used to pre-fracture the gate roof before mining; (c) The advancing support for the working face mining; (d) The temporary supporting for advancing mining during the gob-side entry retaining; (e) The gob-side entry after removing the temporary supporting when the gob -side entry was stabilized.

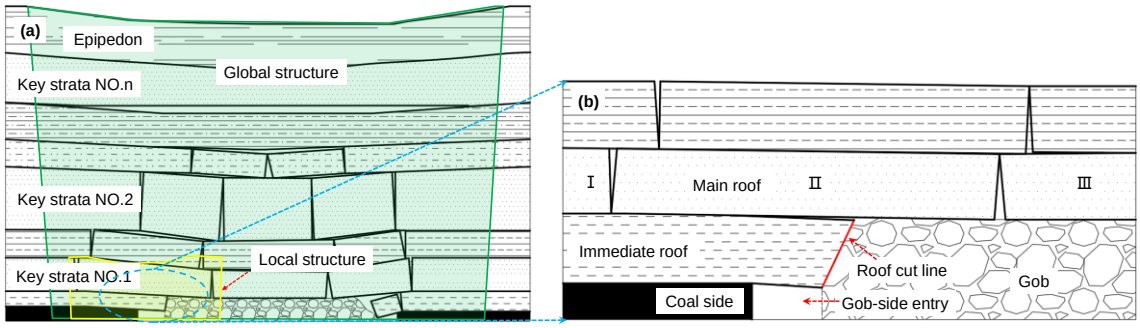

Fig. 3 Structure of overlying strata during gob-side entry retaining: (a) Global structure in the gob-side entry retaining; (b) Local structure.

stability in its life cycle, so the structure model of gob-side entry was established considering the plastic zone of solid coal along the roadside firstly by theoretical analysis. Furthermore, combined FLAC3D and 3DEC, efficient and accurate numerical simulation of large-scale geotechnical engineering design can be realized, and program evaluation can be carried out. Among them, FLAC3D would be used to reveal the stress distribution in stope and get the stress of the roadway surrounding rock after the roof cut. The stress of the roadway surrounding rock would be used to prepare for the boundary condition of the local-discrete model calculated by 3DEC. Finally, we can evaluate the support effect of the local model through 3DEC.

2. Technological process of gob-side entry retaining

2.1 Technological process of gob-side entry formed by roof cut

There is a significant difference between the technology of the GEFRC and the traditional technique of the gob-side entry retaining by roadside packing (He. 2014, Zhang *et al.* 2015). In addition to supporting the roadway surrounding rock in the early stage of roadway excavation (see Fig. 2(a)), roof cut by the directional pre-cracking needs to be carried out before the working face mining (see Fig. 2(b)). Then, during mining, it is necessary to carry out advanced support for the mining roadway (see Fig. 2(c)). After the working face mining, the gangue retaining support along the roof cut line beside the roadway and the support in the gob-side entry are constructed (see Fig. 2(d)). When the gob-side entry is stable, the temporary support of the side and inside the roadway needs to be removed, and the gob-side entry is used when the next working face mining (see Fig. 2(e)).

2.2 Structure character during gob-side entry retaining and using

Before studying the structural model of gob-side entry, concepts of global structure, medium structure and topical structure have to be created first. And global structure contains the medium structure and medium structure contains topical structure (see Fig. 3(a)). Coal seam and all overlying strata are included in the global structure. Also, the strata between the first key layer and the mining coal

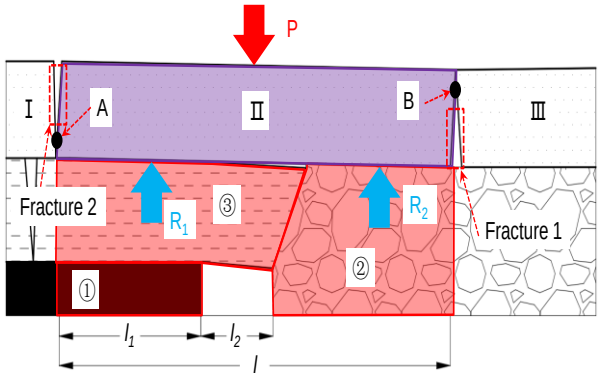

(a) The surrounding rock structure of the gob-side entry

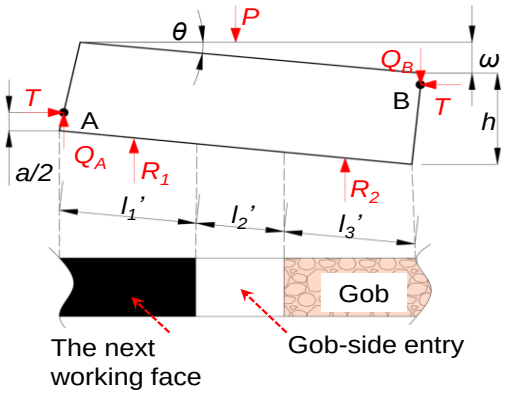

(b) The structural mechanics model of the key block II in the gate surrounding rock

Fig. 4 Structural model of surrounding rock of gob-side entry when working face mining

seam is included in the medium structure. Besides, the small structure only comprises immediately roof, immediately floor and coal side to gob-side entry. According to the existed research results, we can find that mining is the inducement of mining stress, and the load of global structure applied to the local structure is the source of the mining stress. So, as long as the boundary stress applied to the local structure by the medium structure can be grasped, the surrounding rock stability of the gob-side entry can be analyzed. And we can focus on the local structure to analyze their stability during gob-side entry retaining by the discrete element method (see Fig. 3(b)).

2.3 Mechanical models during gob-side entry retaining and using

In the process of the GEFRC, the roadway roof has been pre-split directionally before the working face mining. Therefore, that is why the gob roof would quickly collapse and provides effective support to the basic roof after mining. Under the influence of the mining stress, the key layer fracture first at 'fracture 1', and formed key block III (see Fig. 4(a)). Since the initial stiffness of the gravel side is less than the stiffness of the coal side, the key layer above the coal side generates greater tensile stress due to the rotational deformation of the rock block. When the maximum tensile stress in the basic roof is greater than its tensile strength, two fractures occur at the top of the coal side, and key blocks I and II are formed. The key block II is not only the bearing body of the overburden load of the overlying strata but also the carrier that transfers the overburden load to the roadway surrounding rock. The gravel side and the coal side are the bearing bodies. Therefore, key block II is the decisive rock block structure for the stability of the surrounding rock of the gob-side entry.

The surrounding rock structure of the gob-side entry is formed by the coal side '①', the gravel side '②', the cantilever beam '③' and the roadway floor. In the process of gob-side entry retaining, the coal side '①', the gravel side '②' and the cantilever beam '③' jointly form the support for the key block II, thereby maintaining the stability of the overall structure of the roadway surrounding rock. Therefore, if the overburden load P is known, the roadway surrounding the rock model can be solved. When the limit equilibrium state is assumed, the supporting forces of the coal side '①' and the gravel side '②' to the roof are R_1 and R_2, respectively (see Fig. 4(a)).

According to the voussoir beam theory, the action point of the horizontal thrust stress T is at $h/4$, that is, $h=2a$ (see Fig. 4(b)). So

$$T = \frac{Pl}{h} \tag{1}$$

$$Q_A = Q_B = \frac{Plsin\theta}{4h} \tag{2}$$

In the formula, l is the length between Fracture 1 and Fracture 2, and h is the thickness of the key layer, and Q_A and Q_B are the frictional shear at the contact points of A and B in Fig. 4(b), respectively. And θ is the rotation angle of the key block II, and P is the load exerted on key block II by the overlying rock layer, namely.

$$P = \sum_{i=1}^{i=n} \gamma_i h_i \tag{3}$$

In the formula, Υ_i is the bulk density of the i-th layer in the overburden, kg/m^3, and h_i is the thickness of the i-th layer, and n is the n-th layer of the overlying rock from the key block II.

Due to the strong compressibility of the gravel side, the key block II may fracture during the process of rotation and deformation. So its length is similar to the periodic weighting length of the working face. Therefore, it can be known from the mechanics of materials.

$$l = \frac{2R_T \cdot h^2}{P} \tag{4}$$

In the formula, R_T is the tensile strength.
So

$$l_3 = l - l_1 - l_2 \tag{5}$$

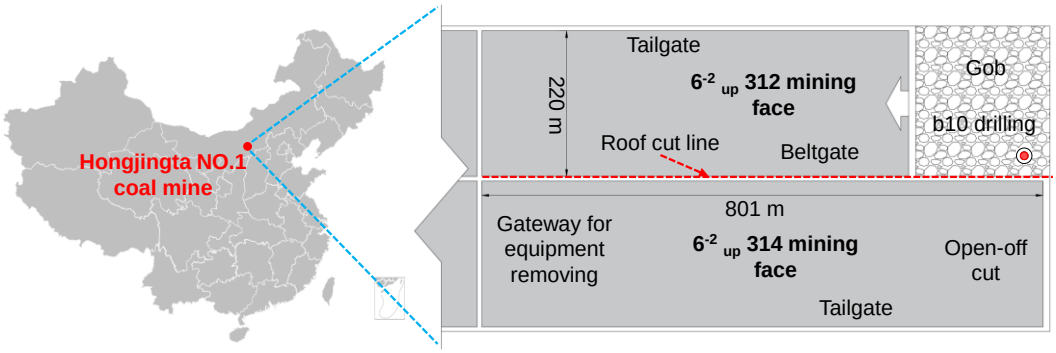

Fig. 5 Relative position of Hongjingta No. 1 coal mine and the 6-2up 312 working face

And because the position of the 'Fracture 2' above the coal side is at the elastoplastic junction of the key layer, it can be known from the theory of elasticity that

$$l_1 = \frac{M_C \lambda}{2tan\varphi_0}\left[\frac{k\gamma H + \frac{c_0}{tan\varphi_0}}{\frac{c_0}{tan\varphi_0} + \frac{p_x}{\lambda}}\right] \tag{6}$$

In the formula, M_C is the thickness of mining; λ is the lateral pressure coefficient; and k is the stress concentration coefficient; and p_x is the support strength of the coal side, MPa; and H is the buried depth of the roadway, m; and c_0 is the bond strength of the coal and rock; and φ_0 is the internal friction angle of the coal and rock; and λ is the average density of the overburden, kg/m^3 ; and k is the stress concentration factor.

$$\theta = arcsin(\omega/l) \tag{7}$$

In the formula, ω is the displacement of B point in the vertical direction in Fig. 2.

As shown in Fig. 4(b), it can be obtained by the static balance principle

$$R_1 = \frac{P[sin\theta \cdot l^2 + 2h(l - l_1) - 4l]}{2h(l + l_2)} \tag{8}$$

$$R_2 = \frac{P[2h(l - l_3) - sin\theta \cdot l^2 + 4l]}{2h(l + l_2)} \tag{9}$$

Therefore, in the process of the GEFRC, timely increasing the strength of the gob-side support (which is R_2) is one of the key factors to avoid roof rock fracture and control the stability of the surrounding rock of the gob-side entry.

3. Engineering geological conditions and molding methods

3.1 Field Engineering Background

Hongjingta No. 1 Coal Mine is located in the Shenfu-Dongsheng Coalfield, the largest coalfield proven in China. Due to the simple geological structure in the hinterland of the Ordos Basin, folds and faults are not developed, so the coal seams are well-occurring. The 6-2$_{up}$312 working face in the 6# coal seam adopts the comprehensive mechanized coal mining method with strike backward. The inclined length of the working face is 220 m, and the strike length is 801 m (see Fig. 5). As the beltgate will experience the influence of the mining pressure many times during the gob-side entry retaining, whether the original support of the roadway can meet the requirements of the roadway must be carefully analyzed and demonstrated before construction.

The average buried depth of the 6-2$_{up}$312 working face is 85.66 m, and the beltgate is the reserved roadway, which is used as the beltgate of the 6-2$_{up}$314 working face after the gob-side entry retaining. The beltgate is a rectangular roadway with a clear width of 4.5 m and a clear height of 2.3 m. The average thickness of the coal seam is 1.85 m, and the inclination angle of the coal seam is 10 ~ 20. The direct roof is composed of 4.3 m sandy mudstone and 0.6 m carbonaceous mudstone. Above the carbonaceous mudstone is 2.75 m mudstone, and above the mudstone is the fine sandstone with a thickness of 3.83 m. The direct floor of the coal seam is sandy mudstone with a thickness of 0.6 m, and the main floor is sandstone with a thickness of 2.35 m. The sandstone contains a small number of carbon chips and muddy interstitials (see Fig. 6). And the physical and mechanical parameters of each rock layer are shown in Table 1.

3.2 Molding methods

To accurately and quickly carry out the numerical analysis and evaluation of the roadway support design in the process of the GEFRC, the method of combining FLAC-3D and 3DEC was adopted to evaluating the support effect of the gob-side entry based on the technical characteristics of the GEFRC. FLAC-3D would be used to reveal the stress distribution in stope and get the stress of surrounding rock after roadway excavation and roof cut. The stress of surrounding rock would be used to prepare for the boundary condition of the local-discrete model. Finally, the local discrete element model was used to simulate and analyze the roadway support effect during the gob-side entry retaining, so as to optimize the roadway support design before mining.

First, according to the engineering geological conditions, the simulation range, engineering rock group, boundary conditions, etc. were determined. And FLAC-3D software was used to build a calculation model consistent with the field conditions. The model size was 300 m ×

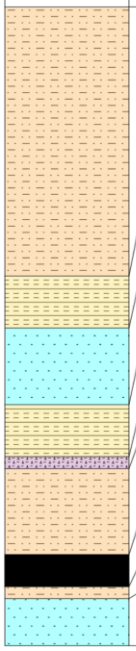

Column	Lithology	Thickness/m	Gross thickness/m	Characteristics
	Sandy mudstone	13.45	69.73	
	Mudstone	2.60	72.33	
	Sandstone	3.83	76.16	Main roof
	Mudstone	2.60	78.91	Immediate roof
	Carbon mudstone	0.60	79.51	
	Sandy mudstone	4.30	83.81	
	Coal	1.60	85.66	Coal with layered structure
	Sandy mudstone	0.60	86.26	Immediate floor
	Sandstone	2.35	88.61	Main floor

Fig. 6 Comprehensive histogram of the 6-2$_{up}$312 working face

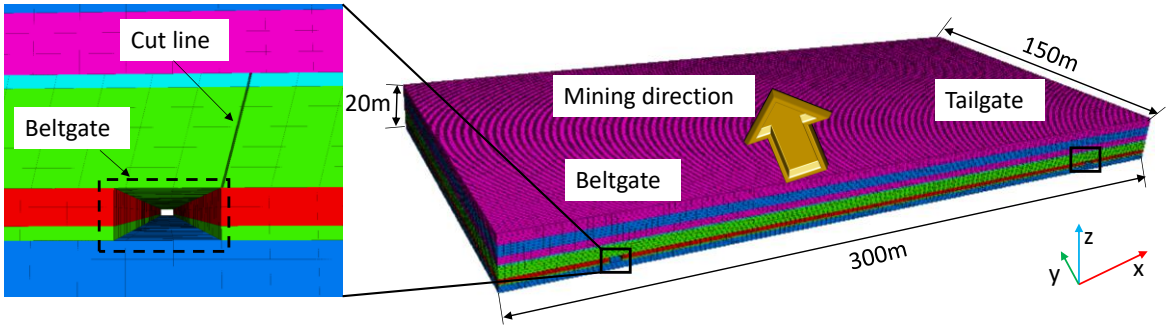

Fig. 7 Global model diagram

Table 1 Physical and mechanical parameters of coal and rock

Lithology	Density/(kg·m^{-3})	Bulk modulus/GPa	Shear modulus/GPa	Compressive strength/Mpa	Cohesive /Mpa	Internal friction angle/(°)
Sandstone	2660	26.4	10.8	69.1	66.2	41.6
Sandy mudstone	2470	20.2	8.1	42.7	38.3	33.2
Carbon mudstone	2320	17.5	6.5	22.5	23.8	26.2
mudstone	2430	16.6	6.2	31.4	27.6	31.0
Coal	1280	7.3	2.7	16.9	16.7	21.5

150 m × 20 m (see Fig. 7). The beltgate width and height were 4.5 m and 2.3 m. It was tunneled along the roof of the coal seam. Its roof cut depth was 5.0 m, and the angle between the roof cut line and the plumb line was 150. The model adopted the Mohr-Coulomb strength criterion, the front and back and left and right boundary displacements were fixed in the x-y direction, the upper boundary was free, the bottom boundary was fixed support, and the upper boundary applied a vertical downward compensation load F_z = 1.38 MPa. Besides, the model grid size was 1 m * 1 m, and the number of cells was 538,200.

In the process of numerical simulation with FLAC-3D, the two construction steps of mining gates excavation and roof cut were carried out. After the calculation, the stress distribution diagrams of the sections x-z, x-y and y-z along the direction perpendicular to the section were taken at x = 45 m, z = 18 m and y = 50 m (see Fig. 8). The numerical simulation results shown that the horizontal stress qy of the section x-z along the y-direction was 1.45 MPa (see Figs.8(a) – 8(c)), and the vertical stress of the section x-y along the z-direction q_z = 1.38 MPa (see Fig. 8(d)), the horizontal stress q_x of the section y-z along the x-direction was 1.46 MPa (see Fig. 8(e)).

Considering that the periodic weighting length of the adjacent working face was about 20 ~ 30 m, the local model size was selected as 45 m × 150 m × 18 m (Fig. 9). The unit

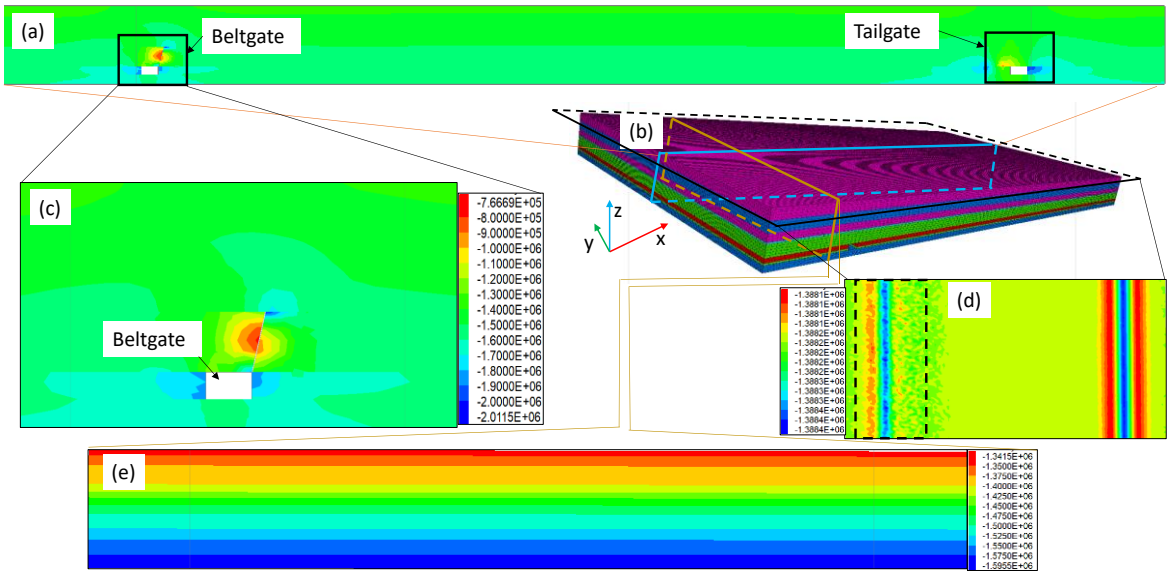

Fig. 8 Stress distribution diagram of the global model: (a) Horizontal stress distribution diagram of the x-z section along the y coordinate axis. (b) Global model diagram. (c) Horizontal stress distribution diagram along the x-z section of the beltgate along the y coordinate axis. (d) Vertical stress distribution diagram of the x-y section along the z coordinate axis. (e) Horizontal stress distribution diagram of the y-z section along the x coordinate axis. (Units in the drawing : MPa)

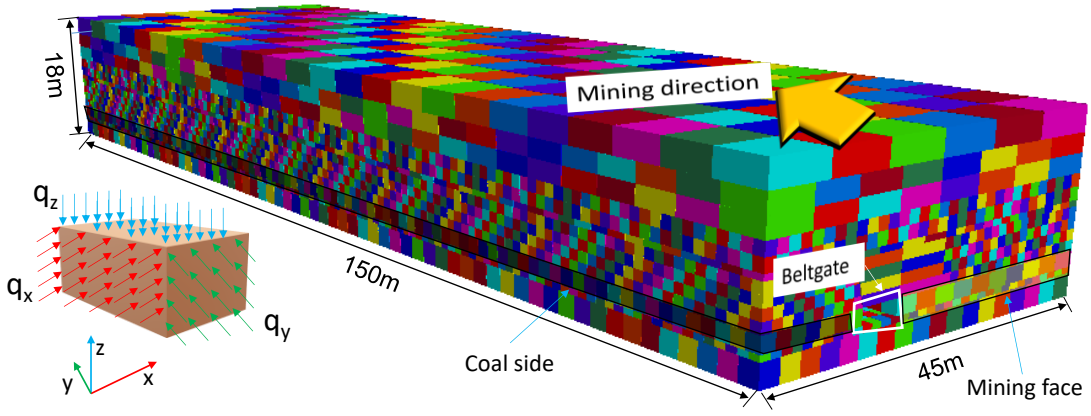

Fig. 9 Local model diagram

block in the model was a cube. The total number of blocks was 31473. And the number of joints was 970189. The displacement of the front and back and left and right boundaries of the local model was fixed in the x-y direction. According to the calculation results of the global model, the horizontal load q_y = 1.45 MPa was applied to the front and rear boundaries. And the horizontal load q_x = 1.46 MPa was applied to the left and right boundaries. And the vertical downward compensation load q_z = 1.38 MPa was applied to the upper boundary. And the bottom boundary was fixed support.

3.3 Support design

Based on the local model diagram, it was carried out to the analysis and evaluation of the roadway support effect of different support methods. There were two support design schemes, scheme A is the original support of the roadway, and scheme B was the reinforcement support scheme. Scheme A adopted “bolt + steel mesh” support, and the main support unit was steel bolt: Φ18 mm * 1.8 m (see Fig. 10(a)). The row spacing between bolt was 1.3 m*1.2 m. The roof cut height was 5.0 m. And the angle between the cutting line and the plumb line was 150. Scheme B adopted “bolt + constant resistance large deformation (CRLD) cable + steel mesh” support (see Fig. 10(b)). The size of the steel bolt was Φ18 mm * 1.8 m. And the row spacing was 1.3 m * 1.2 m. The size of the CRLD cable was Φ22 mm * 7.3 m. And the row spacing was 1.75 m * 1.20 m. The angle between the roof cut line with a roof cut height of 5 m and the plumb line was 150. In the process of the GEFRC, each mining length was 10 m. And the model adopted the Mo-Coulomb strength criterion. At the same time, in the process of numerical calculation, three displacement measuring points were arranged on the surface of the roadway roof to monitor the roof sink, and four measuring points were arranged at different depths of the coal side to monitor the deformation of the coal side during the process of the GEFRC (see Fig. 11).

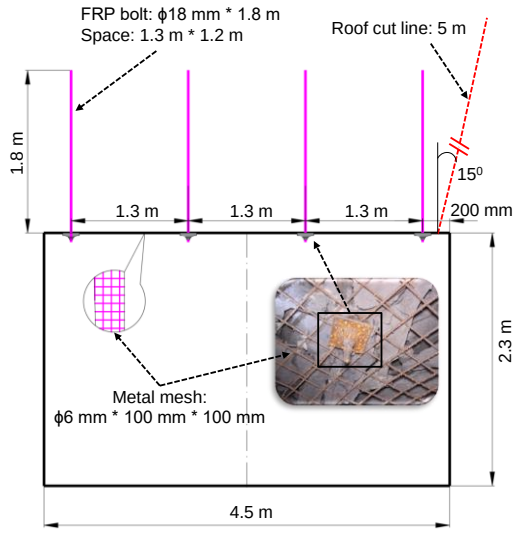

(a) Cross-sectional view of the support design of scheme A

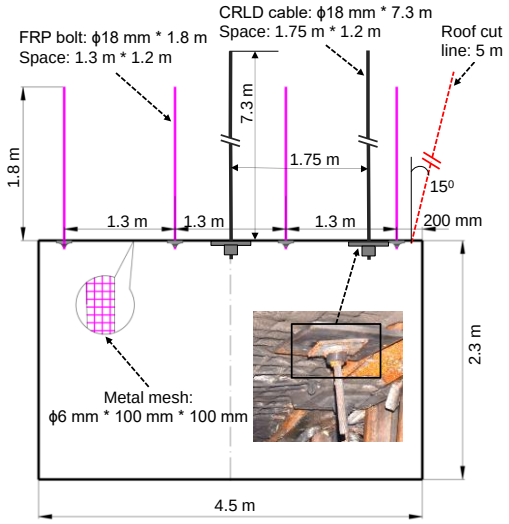

(b) The cross-sectional view of the support design of scheme B

Fig. 10 Cross-section view of the support in the beltgate

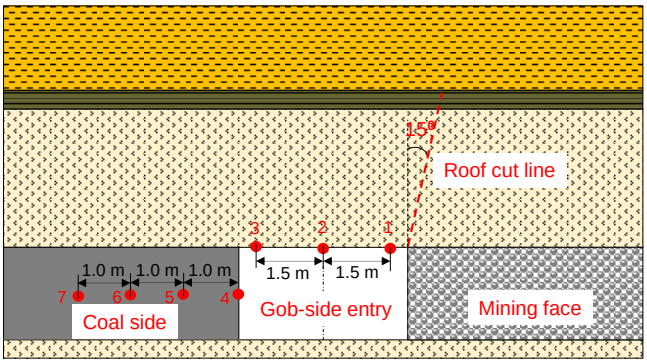

Fig. 11 Layout of displacement monitoring points

3.4 Numerical simulation results

Numerical simulation results shown that when the supporting form of Scheme A was adopted for the beltgate. The stress concentration of the roof along the cut line side was not obvious with the coal mining, but the coal side and its upper roof formed a width of about 1.5 m arc-shaped stress concentration zone (see Fig. 12(a)). When the working face was 10 m ahead, the range of the stress concentration zone did not change much. But the upper roof stress of the coal side increased little (see Fig. 12(b)). After coal mining, the range and strength of the arc-shaped stress concentration area suddenly increased. And the range of the stress concentration area was inclined to the roof of the gob-side entry (see Fig. 12(c)). When the distance of the lagging mining face was 50 m, the arc-shaped stress concentration area was reduced. And the stress concentration above the roof of the gob-side was greatly reduced (see Fig. 12(d)). With the further increase of the distance of the lagging mining face, the range of the arc-shaped stress concentration area was reduced to the range of the coal side and its upper strata (see Figs.12(e) ~ 12(f)).

When the working face was 20 m ahead, due to the influence of the leading support pressure, the roadway roof began to deform. The roof deformation along the gob side was the largest while the roof deformation on the coal side was the smallest. As the distance from the working face decreases, the roadway roof deformation increased slightly (see Figs.13(a) – 13(b)). After the coal mining, the roadway roof deformation and bed separation along with the goaf increased rapidly (see Fig. 13(c) – 13(d)). When 90 m lagging the working face, uncoordinated deformation of the roadway roof along the goaf occurred. And the roadway roof deformed in an arc shape (see Fig. 13(e)). When 120 m lagging the working face, the roadway roof fractured along the middle of the roadway. Finally, an angle of 150^0 formed between the roadway roof along the coal side and the roadway roof along the cut line side (see Fig. 13(f)).

When the beltgate adopted the support design of scheme A the stress of measuring point ‘1’ and measuring point ‘2’ on the roadway roof did not change much during the gob-side entry retaining. When measuring point ‘3’ was 22.5 m ahead of the working face, the stress gradually increased. And when lagging the working face 83 m, the growth rate slowed down. And when lagging the working face by 120 m, it was stable at 4.5 MPa (see Fig. 14(a)). The stress of measuring point ‘5’ ~ ‘7’ on the coal side did not change much during the process of gob-side entry retaining. The stress of measuring point ‘4’ increased gradually when the working face was 15 m ahead. And the stress increased sharply when lagging the working face by 15 m. And when lagging the working face by 60 m it slowed down and stabilizes at 9.5 MPa when the lagging working face was 120 m (see Fig. 14(b)). The displacement of measuring point ‘1’ on the roadway roof did not change much during the process of gob-side entry retaining. When measuring points ‘2’ and ‘3’ were 30 m ahead of the working face, the deformation gradually increased. And when lagging the working face by 83 m, the deformation tended to be slower. The roadway roof deformation tended to be stable when the lagging working face was 120 m. And the maximum roof subsidence of measuring point ‘2’ and measuring point ‘3’

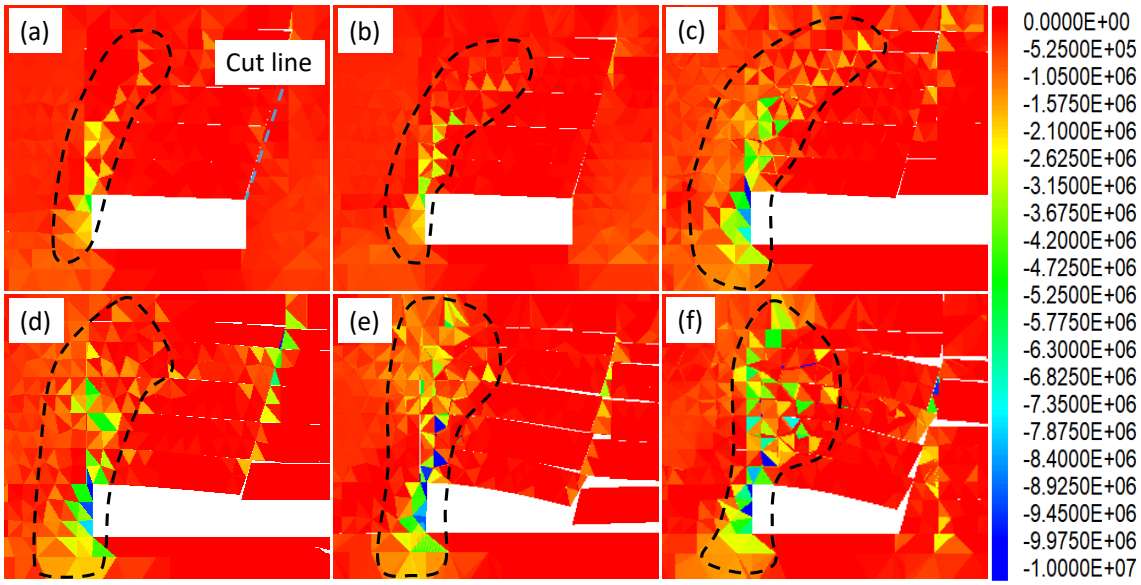

Fig. 12 Vertical stress distribution diagram of the roadway surrounding rock in Scheme 1: (a) Stress distribution diagram 20 m ahead of the working face. (b) Stress distribution diagram 10m ahead of the working face. (c) Stress distribution diagram 10m lagging the working face. (d) Stress distribution diagram 50 m lagging the working face. (e) Stress distribution diagram 90m lagging the working face. (f) Stress distribution diagram 120m lagging the working face. (Units in the drawing : MPa)

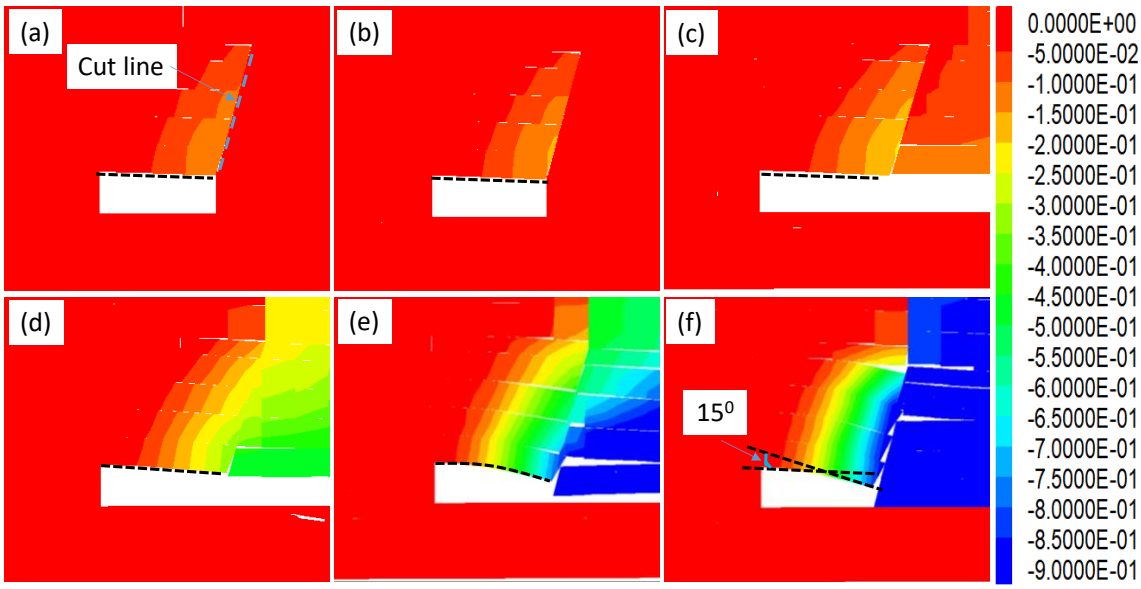

Fig. 13 Displacement distribution diagram of the roadway surrounding rock in scheme 1: (a) Displacement distribution diagram 20 m ahead of the working face. (b) Displacement distribution diagram 10 m ahead of the working face. (c) Displacement distribution diagram 10 m lagging the working face. (d) Displacement distribution diagram 50 m lagging the working face. (e) Displacement distribution diagram 90 m lagging the working face. (f) Displacement distribution diagram 120 m lagging the working face. (Units in the drawing : mm)

was 300 mm and 900 mm, respectively (see Fig. 14(c)). The displacement of each measuring point in the coal side did not change much. And the maximum displacement of measuring point '4' with the most significant displacement was only 9.5 mm (see Fig. 14(d)).

When the beltgate adopted the supporting form of scheme B, with coal mining, the coal side and its upper roof formed an arc-shaped stress concentration zone with a width of about 1.5 m (see Fig. 15(a)). When the working face was 10 m ahead, the stress in the range of the stress concentration area increased (see Fig. 15(b)). After coal mining, the range and strength of the arc-shaped stress concentration area continued to increase while the range of the stress concentration area sloped toward the roof of the gob side (see Figs.15(c) – 15(d)). When 90 m lagging the working face, the arc-shaped stress concentration area was further enlarged. Because the roadway roof was reinforced and supported by CRLD cables, the coal side and the roadway roof formed an inverted "J"-shaped stress-bearing area (see Figs.15(e) – 15(f)).

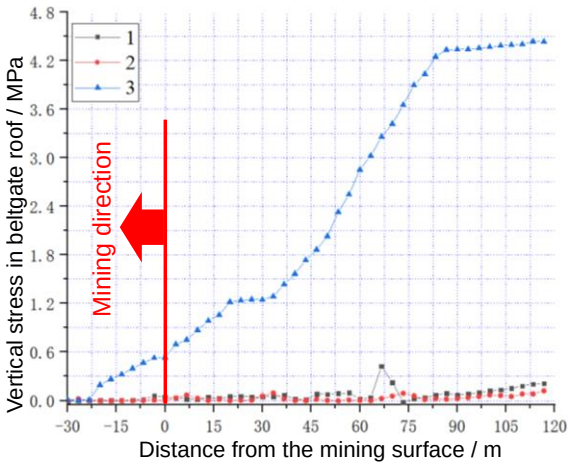

(a) Stress curve of the measurement point of the roadway roof

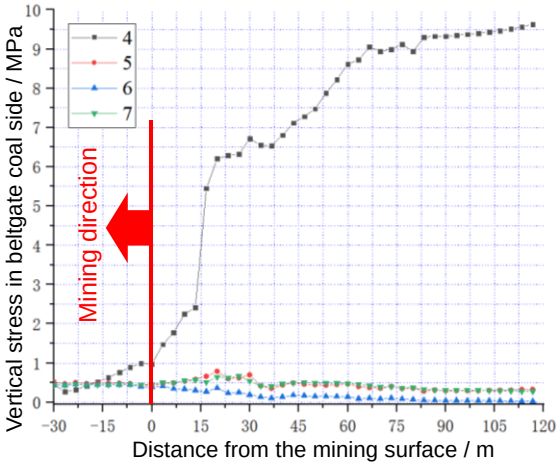

(b) Stress curve of the measurement point on the coal side

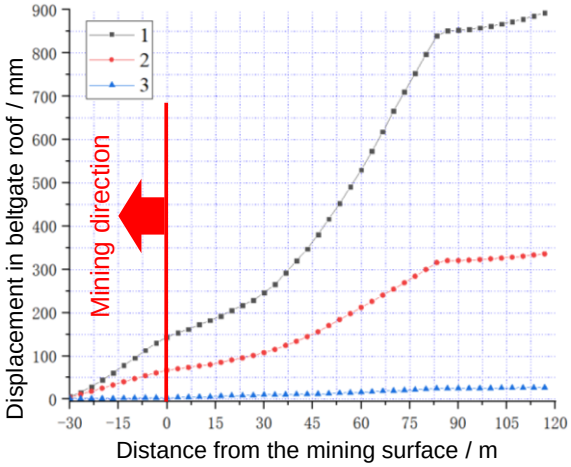

(c) Displacement curve of the measurement point of the roadway roof

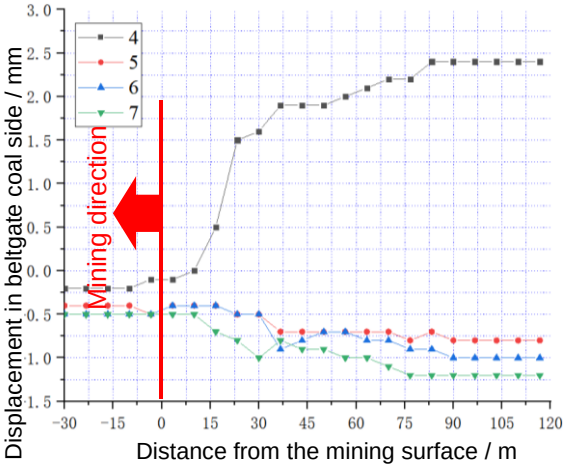

(d) Displacement change curve of the measurement point on the coal side

Fig. 14 The stress and displacement curve of the measuring point of the roadway surrounding rock in Scheme 1

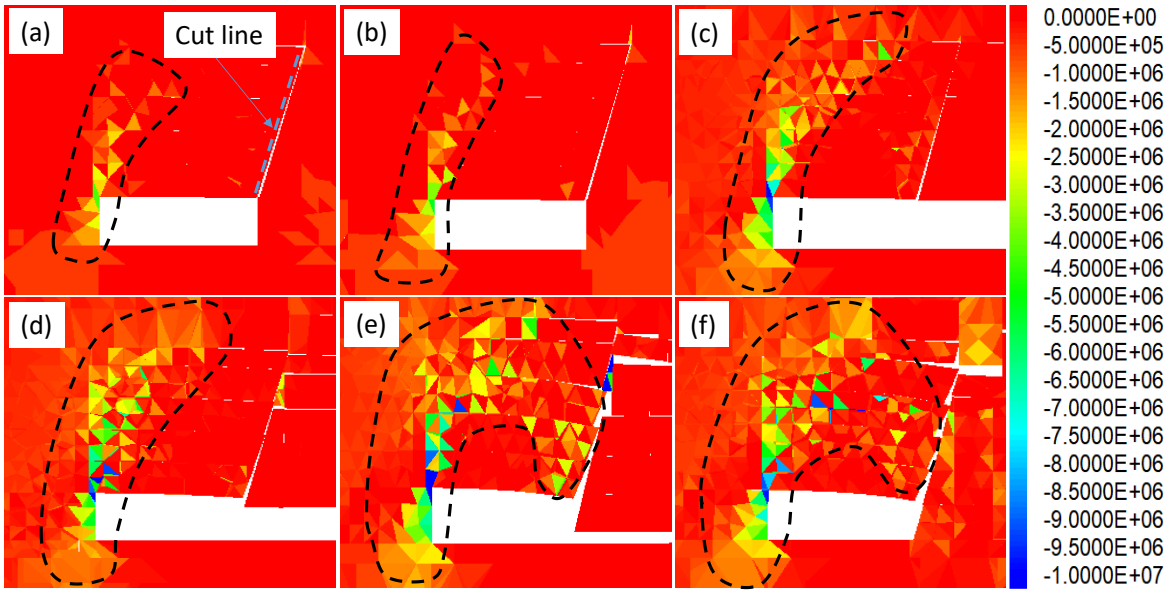

Fig. 15 Vertical stress distribution diagram of the roadway surrounding rock in Scheme 2: (a) Stress distribution diagram 20 m ahead of the working face. (b) Stress distribution diagram 10 m ahead of the working face. (c) Stress distribution diagram 10 m lagging the working face. (d) Stress distribution diagram 50 m lagging the working face. (e) Stress distribution diagram 90 m lagging the working face. (f) Stress distribution diagram 120 m lagging the working face. (Units in the drawing : MPa)

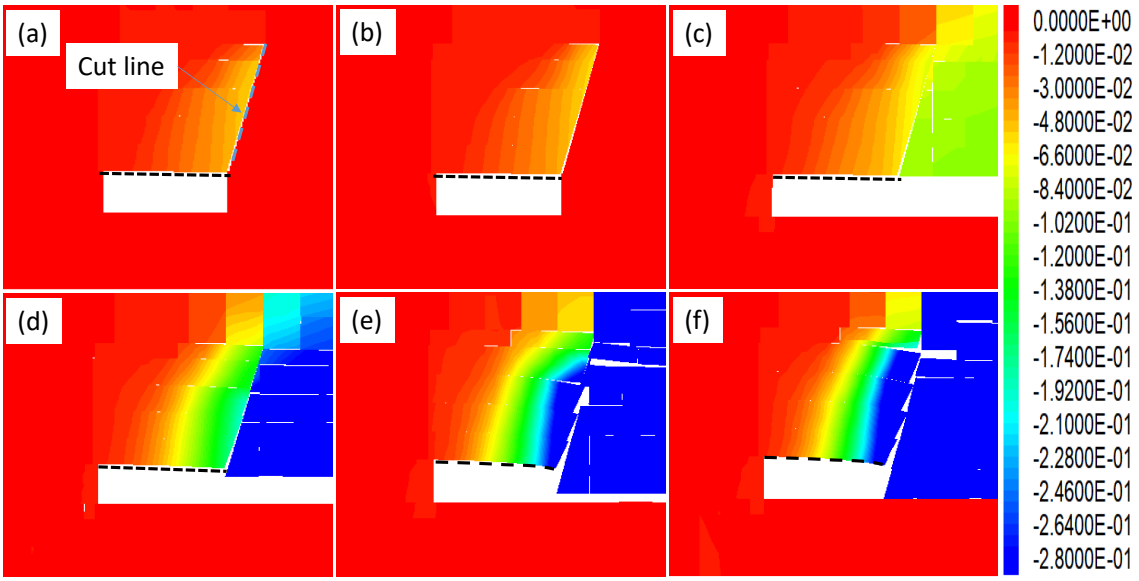

Fig. 16 Displacement distribution diagram of the roadway surrounding rock in scheme 2: a The displacement distribution diagram 20m ahead of the working face. b The displacement distribution diagram 10m ahead of the working face. c The displacement distribution diagram 10m lagging the working face. d The displacement distribution diagram 50m lagging the working face. e The displacement distribution diagram 90m lagging the working face. f The displacement distribution diagram 120m lagging the working face. (Units in the drawing : mm)

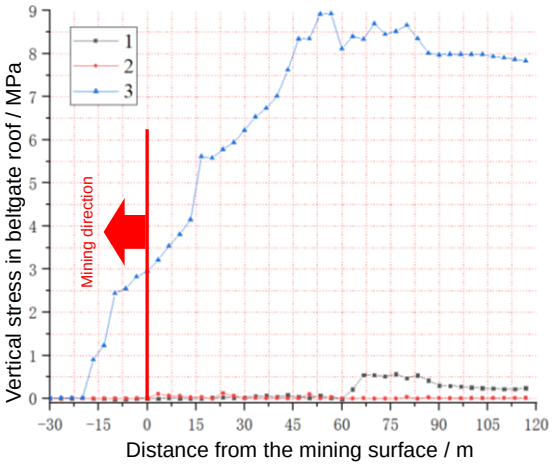

(a) The stress curve of the measurement point of the roadway roof

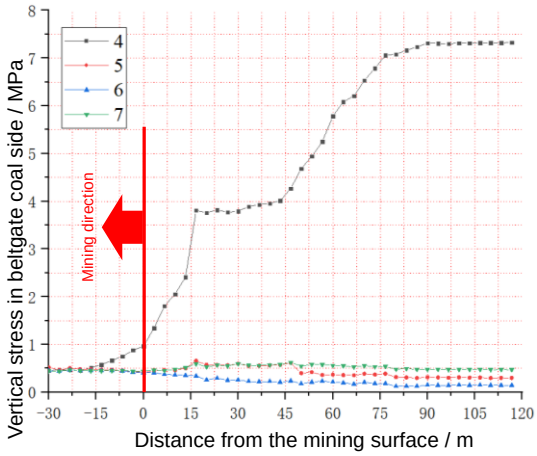

(b) The stress curve of the measurement point on the coal side

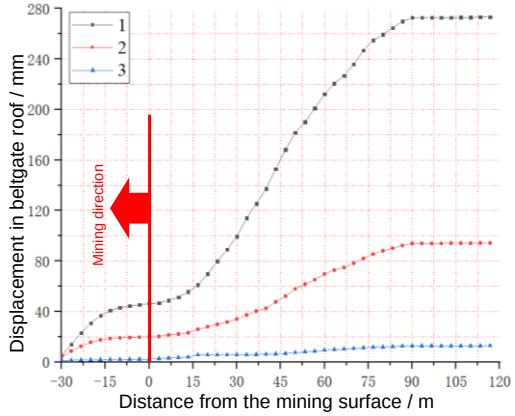

(c) The displacement curve of the measurement point of the roadway roof

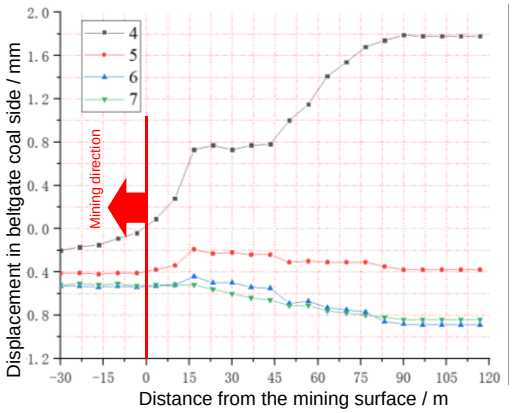

(d) The displacement change curve of the measurement point on the coal side

Fig. 17 The stress and displacement curve of the measuring point of the roadway surrounding rock in Scheme 2

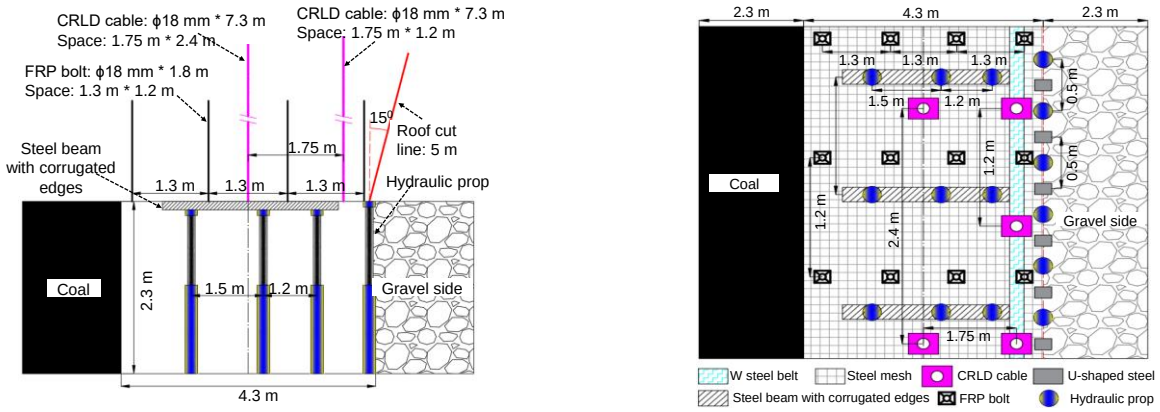

(a) The sectional drawing of support design (b) The plane development drawing of support design

Fig. 18. Support design of the beltgate

Due to the influence of the front abutment pressure and the roof cut, the roadway roof began to undergo rotational deformation with the upper strata of the non-cut seam side as the fulcrum. The roof deformation on the roof cut side was the largest while the roof deformation on the coal side was the smallest (see Figs.16(a) – 16(d)). With continuous coal mining, the deformation of the roadway roof gradually increased. When the lagging the working face was 90 m, the roadway roof along the gob had a bending deformation. The roadway roof deformed in an arc shape. But no fracture occurred (see Figs.16(e)–16(f)). At this time, the deformation of the surrounding rock of the gob-side entry had stabilized.

The stress at the measurement point '3' on the roadway roof had a significant change when the roadway adopted the support form of scheme B. Its stress began to increase gradually at 22.5 m ahead of the working face and reached the maximum value of 9 MPa lagging the working face by 53 m, and then stabilize at 8 MPa lagging the working face by 85 m (see Fig. 17(a)). The stress of measuring point '4' on the coal side changed significantly during the process of gob-side entry retaining. It began to increase gradually at 15 m ahead of the working face. And when lagging the working face by 15 m, the stress increased sharply. When lagging the working face by 90 m, it stabilized at 7.3 MPa (see Fig. 17(b)). The displacement of measuring point '1' on the roadway roof changed little during the process of gob-side entry retaining. But measuring point '2' and measuring point '3' began to deform when they are 30 m ahead of the working face, and stabilize at 273 mm and 78 mm respectively when they lagged the working face by 90 m (see Fig. 17(c)). Same as scheme A, the displacement of each measuring point in the coal side has little change. The displacement of measuring point '4' with the most significant displacement was stable at 1.8 mm when lagging the working face by 90 m (see Fig. 17(d)).

4. Verification of the used approach

According to the results of the numerical simulation, the supporting form of Scheme B was adopted to support the beltgate of the 6-2up312 working face. To ensure the

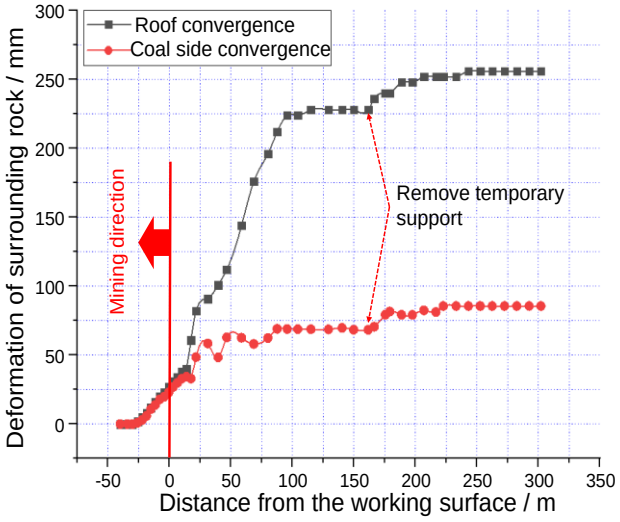

Fig. 19 Deformation of surrounding rock during the gob-side entry retaining

stability of the surrounding rock of the gob-side entry in the dynamic pressure zone, a coordinated support scheme of "CRLD cable + steel bolt + hydraulic prop + steel beam with corrugated edges+ U-shaped steel" was proposed (see Fig. 18(a)). Before mining, the roadway roof adopted the combined support method of "CRLD cable + steel bolt + steel mesh + W steel belt". After the coal mining, the " hydraulic prop + steel beam with corrugated edges " was used for temporary support in the dynamic pressure zone of the gob-side entry. And then the " hydraulic prop + U-shaped steel + diamond mesh" was used for gangue retaining support on the gravel side (see Fig. 18(b)). After the gob-side was stabilized, temporary supports such as hydraulic prop and steel beam with corrugated edges could be removed.

The field test results shown that in the process of the GEFRC, the roadway roof and coal side began to deform when the leading working face is 26 m. The deformation of the roadway surrounding rock speeded up when the lagging working face was 17 m. And the deformation of the roadway surrounding rock reached initial stabilization when the lagging working face was 96 m. At this time, the roof deformation was 224 mm. And the coal side deformation

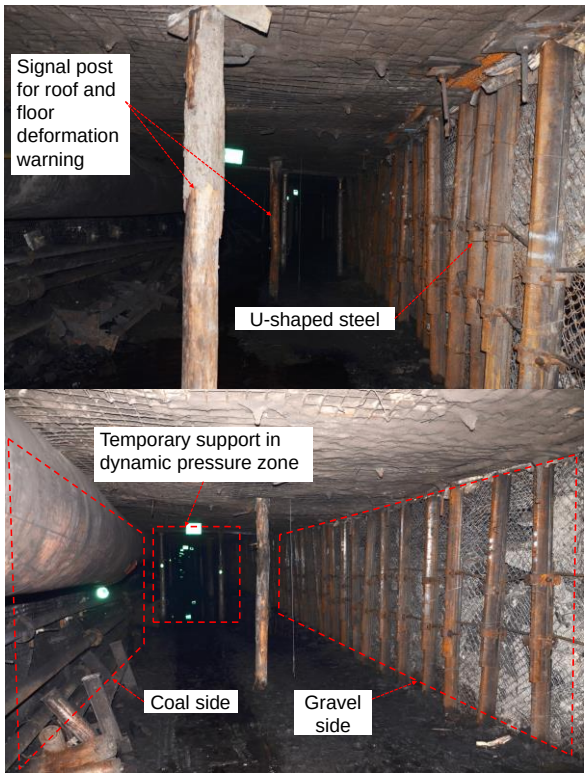

Fig. 20 Effect of the gob-side entry retaining

was 69 mm. When the lagging working face was 162 m, the temporary supports such as single pillars and lace beams were removed. And the roadway surrounding rock undergone secondary deformation. But the deformation speed was relatively slow. When the lagging working face was 243 m, the surrounding rock deformation of the goaf roadway stabilized again. Finally, the roof deformation was 256 mm. And the coal side deformation was 85.6 mm (see Fig. 19). After the gob-side entry was stable, the normal using could be guaranteed when the next working face mining (see Fig. 20).

5. Discussions

The discreteness of rock and soil has an important impact on the accuracy of numerical simulation results in geotechnical engineering. Therefore, the using of finite element software to numerically simulate engineering problems encountered in geotechnical engineering has its own limitations. However, when using the universal distinct element code to numerically simulate engineering problems encountered in geotechnical engineering, the large scale of the engineering model and a large number of joints and block divisions often make numerical calculations difficult.

To solve the above problems, this research used the finite element software FLAC-3D to simulate the global model of the mining stope and its overlying rock, and obtained the stress of the beltgate surrounding rock in the 6-2_{up}312 working face. Then, the universal distinct element code 3DEC was used to carry out a numerical simulation on the process of gob-side entry retaining under different supporting forms to evaluate the supporting effect of different supporting forms.

The research results shown that based on the technological characteristics of gob-side entry retaining, by combining FLAC-3D and 3DEC, not only could the numerical calculation efficiency be improved, but also the accuracy of the numerical simulation could be improved. Field test results and the numerical simulation results were in good agreement. Besides, the numerical simulation results of different supporting forms shown that the support using the high-prestress CRLD cable could greatly improve the integrity and bearing capacity of the surrounding rock of the gob-side entry. The supporting form would not only aggravate the deformation and destruction of the gob-side entry but also easily cause the stress concentration of the coal side, which would cause accidents such as roof fall and rockburst.

The field test results shown that the temporary support in the dynamic pressure zone of the gob-side entry played an important role in maintaining the stability of the roadway surrounding rock and controlling the deformation of the gob-side entry. It should be noted that when the gob-side entry reached initial stabilization, the withdrawal of the temporary support would cause the gob-side entry to deform again.

6. Conclusions

In this paper, numerical simulation, theoretical analysis and field tests were used to conduct in-depth research on the adaptability of different supporting forms of the beltgate in the 6-2up312 working face when gob-side entry retaining. The main conclusions were as follows:

(1) Aiming at the characteristics of geotechnical engineering, based on in-depth analysis of the technology of the GEFRC, a global-finite and local-discrete modeling approach was proposed. The field test results were in good agreement with the numerical simulation results, which was indicated that this method could accurately evaluate the roadway support form in the process of the gob-side entry retaining, and provide a reasonable and effective way for the support design and optimization of the gob-side entry.

(2) Numerical simulation results shown that the “steel bolt + CRLD cable” support formed an inverted “J”-shaped stress-bearing area in the surrounding rock of the gob-side entry. This support form could greatly increase the integrity and bearing capacity of the surrounding rock of the gob-side entry under the influence of mining stress. And the bed separation could be reduced effectively.

(3) Based on the numerical simulation of the different supporting forms of the beltgate during the gob-side entry retaining, the collaborative supporting scheme of “CRLD cable + steel bolt + hydraulic prop + steel beam with corrugated edges + U-shaped steel” was proposed. Field test results shown that the maximum subsidence of the roadway roof was 256 mm while the maximum amount of the coal side displacement was 85.6 mm, which was indicated that the support scheme could effectively control the deformation of the surrounding rock during the process of the GEFRC, and could meet the needs of safe production.

Declaration of Competing Interest

The authors whose names are listed immediately below certify that they have NO affiliations with or involvement in any organization or entity with any financial interest (such as honoraria; educational grants; participation in speakers bureaus; membership, employment, consultancies, stock ownership, or other equity interest; and expert testimony or patent-licensing arrangements), or non-financial interest (such as personal or professional relationships, affiliations, knowledge or beliefs) in the subject matter or materials discussed in this manuscript.

Acknowledgements

This work was supported by the National Natural Science Foundation of China (Grant Nos. 51904188, 41702381) and the Open Fund of State Key Laboratory for GeoMechanics and Deep Underground Engineering (SKLGDUEK1821). In addition, thanks to all the people who contributed to the research and the manuscript.

References

Aksoy, C.O, Aksoy, G.G.U., Guney, A., Ozacar, V. and Yaman, H.E. (2020), "Influence of time-dependency on elastic rock properties under constant load and its effect on tunnel stability", *Geomech. Eng.*, **20**(1), 1-7. https://doi.org/10.12989/gae.2020.20.1.001.

Bai, J.B., Shen, W.L., Guo, G.L., Wang, X.Y. and Yu, Y. (2015), "Roof deformation, failure characteristics, and preventive techniques of gob-Side entry driving heading adjacent to the advancing working face", *Rock. Mech. Rock. Eng.*, **48**(6), 2447-2458. https://doi.org/10.1007/s00603-015-0713-2.

Basarir, H., Sun, Y.Y. and Li, G.C. (2019), "Gateway stability analysis by global-local modeling approach", *Int. J. Rock. Mech. Min.*, **113**, 31-40. https://doi.org/10.1016/j.ijrmms.2018.11.010.

Bednarek, L. and Majcherczyk, T. (2020), "An analysis of rock mass characteristics which influence the choice of support", *Geomech. Eng.*, **21**(4), 371-377. https://doi.org/10.12989/gae.2020.21.4.371.

Cheng, Z.B., Pan, W.D., Li, X.Y. and Sun, W.B. (2019), "Numerical simulation on strata behaviours of TCCWF influenced by coal-rock combined body", *Geomech. Eng.*, **119**(3), 269-282. https://doi.org/10.12989/gae.2019.19.3.269.

De Silva, V.R.S. and Ranjith, P.G. (2019), "Intermittent and multi-stage fracture stimulation to optimisefracture propagation around a single injection well for enhanced in-situ leaching applications", *Eng Fract Mech.*, **220**, https://doi.org/10.1016/j.engfracmech.2019.106662.

He, M.C. (2014), "Progress and challenges of soft rock engineering in depth", *Int. J. Coal. Sci. Techno.*, **33**(7), 389-395. https://doi.org/10.13225/j.cnki.jccs.2014.9044.

Huang, B.X., Liu, J.W. and Zhang, Q. (2018), "The reasonable breaking location of overhanging hard roof for directional hydraulic fracturing to control strong strata behaviors of gob-side entry", *Int. J. Rock. Mech. Min.*, **103**, 1-11. https://doi.org/10.1016/j.ijrmms.2018.01.013.

Kim, H.J., Kim, K.H., Kim, H.M. and Shin, J.H. (2018), "Anchorage mechanism and pullout resistance of rock bolt in water-bearing rocks", *Geomech. Eng.*, **15**(3), 841-849. https://doi.org/10.12989/gae.2018.15.3.841.

Qian, M.G., Liao, X.X. and Xu, J.L. (1996), "Theoretical research on key stratum in strata control", *J. Cn. Coal. Society.*, **21**(3), 225-230.

Qin, X.N., Gu, C.S., Shao, C.F., Chen, Y., Vallejo, L., Zhao, E.F. (2020), "Safety evaluation with observational data and numerical analysis of Langyashan reinforced concrete face rockfill dam", *B. Eng. Geol. Environ.*, **79**(7), 3497-3515. https://doi.org/10.1007/s10064-020-01790-2.

Tan, Y.L., Ma, Q., Zhao, Z.H., Gu, Q.H., Fan, D.Y., Song, S.L. and Huang, D.M. (2019), "Cooperative bearing behaviors of roadside support and surrounding rocks along gob-side", *Geomech. Eng.*, **18**(4), 439-448. https://doi.org/10.12989/gae.2019.18.4.439.

Valliappan, V., Remmers, J.J.C., Barnhoorn, A. and Smeulders, D.M.J. (2019), "A Numerical Study on the Effect of Anisotropy on Hydraulic Fractures", *Rock. Mech. Rock. Eng.*, **52**(2), 591-609. https://doi.org/10.1007/s00603-017-1362-4.

Wang, Q., Pan, R., Jiang, B., Li, S.C., He, M.C., Sun, H.B. and Luan, Y.C. (2017), "Study on failure mechanism of roadway with soft rock in deep coal mine and confined concrete support system", *Eng. Fail. Anal.*, **81**, 155-177. https://doi.org/10.1016/j.engfailanal.2017.08.003.

Wu, J.T., Ye, X., Li, J. and Li, G.W. (2019), "Field and numerical studies on the performance of high embankment built on soft soil reinforced with PHC piles", *Comput. Geotech.*, **107**, 1-13. https://doi.org/10.1016/j.engfailanal.2017.08.003.

Xie, S.R., Pan, H., Chen, D.D., Zeng, J.C., Song, H.Z., Cheng, Q. and Li, Y.H. (2020), "Stability analysis of integral load-bearing structure of surrounding rock of gob-side entry retention with flexible concrete formwork", *Tunn. Undergr. Sp. Tech.*, **103**, 103492. https://doi.org/10.1016/j.tust.2020.103492.

Yin, Z.Y., Wang, P. and Zhang, F.S. (2020), "Effect of particle shape on the progressive failure of shield tunnel face in granular soils by coupled FDM-DEM method", *Tunn. Undergr. Sp. Tech.*, **100**, 103394. https://doi.org/10.1016/j.tust.2020.103394.

Zhang, N., Chen, H. and Chen, Y. (2015), "An engineering case of gob-side entry retaining in one kilometer-depth soft rock roadway with high ground pressure", *J. Cn. Coal. Society*, **40**(3), 494-501.

Zhang, S., Zhang, D.S., Wang, H.Z. and Liang, S.S. (2018), "Discrete element simulation of the control technology of large section roadway along a fault to drivage under strong mining", *J. Geophys. Eng.*, **15**(6), 2642-2657. https://doi.org/10.1088/1742-2140/aae052.

Zhu, D.F., Tu, S.H., Ma, H.S., Wei, H.M., Li, H.C. and Wang, C. (2019), "Modeling and calculating for the compaction characteristics of waste rock masses", *Int. J. Numer. And. Anal. Met.*, **43**(1), 257-271. https://doi.org/10.1002/nag.2862.

GC